Supporting Information

Title: **Defective cytokinin signaling reprograms lipid and flavonoid gene-to-metabolite networks to mitigate high salinity in *Arabidopsis***

Mostafa Abdelrahman, Rie Nishiyama, Cuong Duy Tran, Miyako Kusano, Ryo Nakabayashi, Yozo Okazaki, Fumio Matsuda, Ricardo A. Chávez Montes, Mohammad Golam Mostofa, Weiqiang Li, Yasuko Watanabe, Atsushi Fukushima, Maho Tanaka, Motoaki Seki, Kazuki Saito, Luis Herrera-Estrella, and Lam-Son Phan Tran

To whom correspondence may be addressed:
E-mail: Luis.Herrera-Estrella@ttu.edu or son.tran@ttu.edu

This file includes:

Figs. S1-S7
Captions for Datasets S1-S11

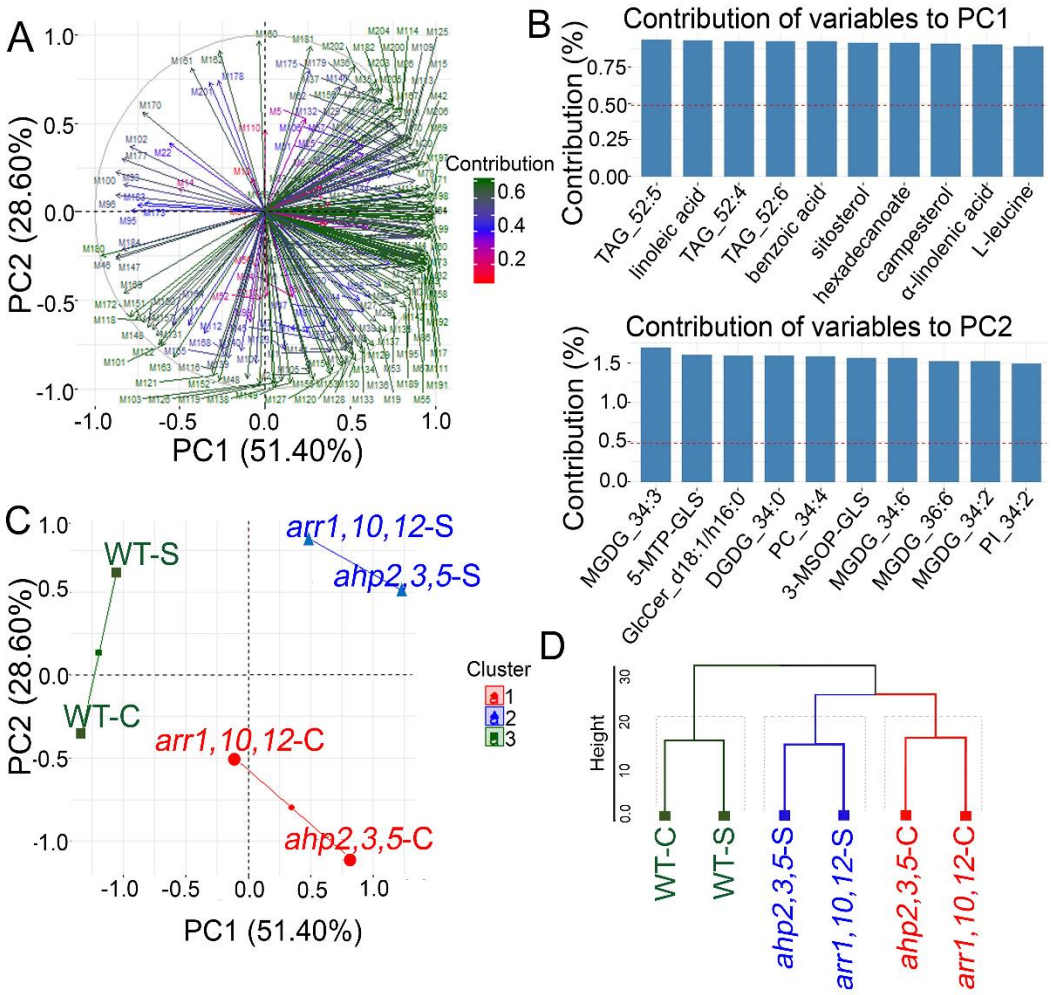

Fig. S1. Principal component analysis (PCA) and dendrogram clustering of the interrelated effects of salt stress on *Arabidopsis* wild-type (WT), and cytokinin-signaling *ahp2,3,5* and *arr1,10,12* mutants. (*A*) PCA-loading plot of all 206 variable metabolites identified in the investigated genotypes grown under nonsaline (WT-C, *ahp2,3,5*-C and *arr1,10,12*-C) and saline (WT-S, *ahp2,3,5*-S and *arr1,10,12*-S) conditions. The contribution of each metabolite to PC1 or PC2 axes was colored based on the contribution color scale. (*B*) Contribution percentages of the top 10 metabolites to PC1 and PC2 axes. (*C*) Dissemination of the genotypes grown under nonsaline and saline conditions as shown by a PCA-score plot constructed based on the 206 metabolite variables. (*D*) Dendrogram clustering of the investigated genotypes grown under nonsaline and saline condition conditions using 206 metabolite variables. The height of the bar indicates the distance between the clusters.

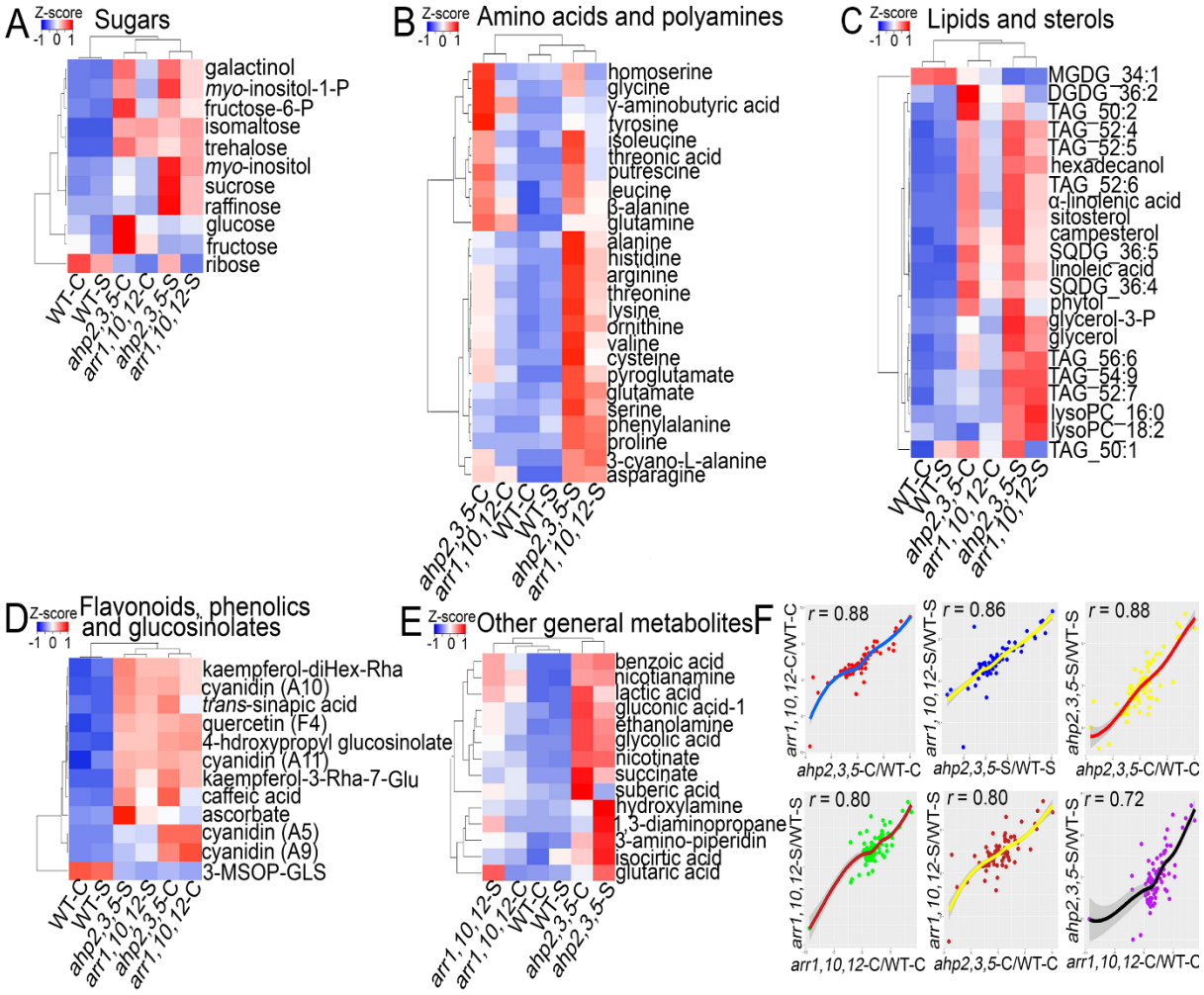

Fig. S2. Heatmap hierarchical clustering and 'genotype-genotype' correlations of 83 metabolites differentially produced in *ahp2,3,5* and *arr1,10,12* mutants, relative to wild-type (WT) plants, grown under nonsaline ('*ahp2,3,5*-C/WT-C' and '*arr1,10,12*-C/WT-C') and saline (*ahp2,3,5*-S/WT-S' and '*arr1,10,12*-S/WT' comparisons) conditions. (*A-E*) Heatmap hierarchical clusters of 83 differentially produced sugars (*A*), amino acids and polyamines (*B*), lipids and sterols (*C*), flavonoids, phenolics and glucosinolates (*D*), and general metabolites (*E*) in the *ahp2,3,5* and *arr1,10,12* mutants and the WT plants under saline and nonsaline conditions. (*F*) 'Genotype-genotype' correlations based on the Pearson correlation coefficient of differentially produced metabolites in the investigated comparisons. The metabolite production levels in the heatmaps are a Z-score-normalized data matrix. Red and blue colors indicate increased and decreased levels of metabolites, respectively, as indicated by the colored scales. Lysophosphatidylcholine, LysoPC; 3-methylsulfinylpropyl glucosinolate, 3-MSOP-GLS; monogalactosyldiacylglycerol, MGDG; sulfoquinovosyl diacylglycerol, SQDG; triacylglycerol, TAG.

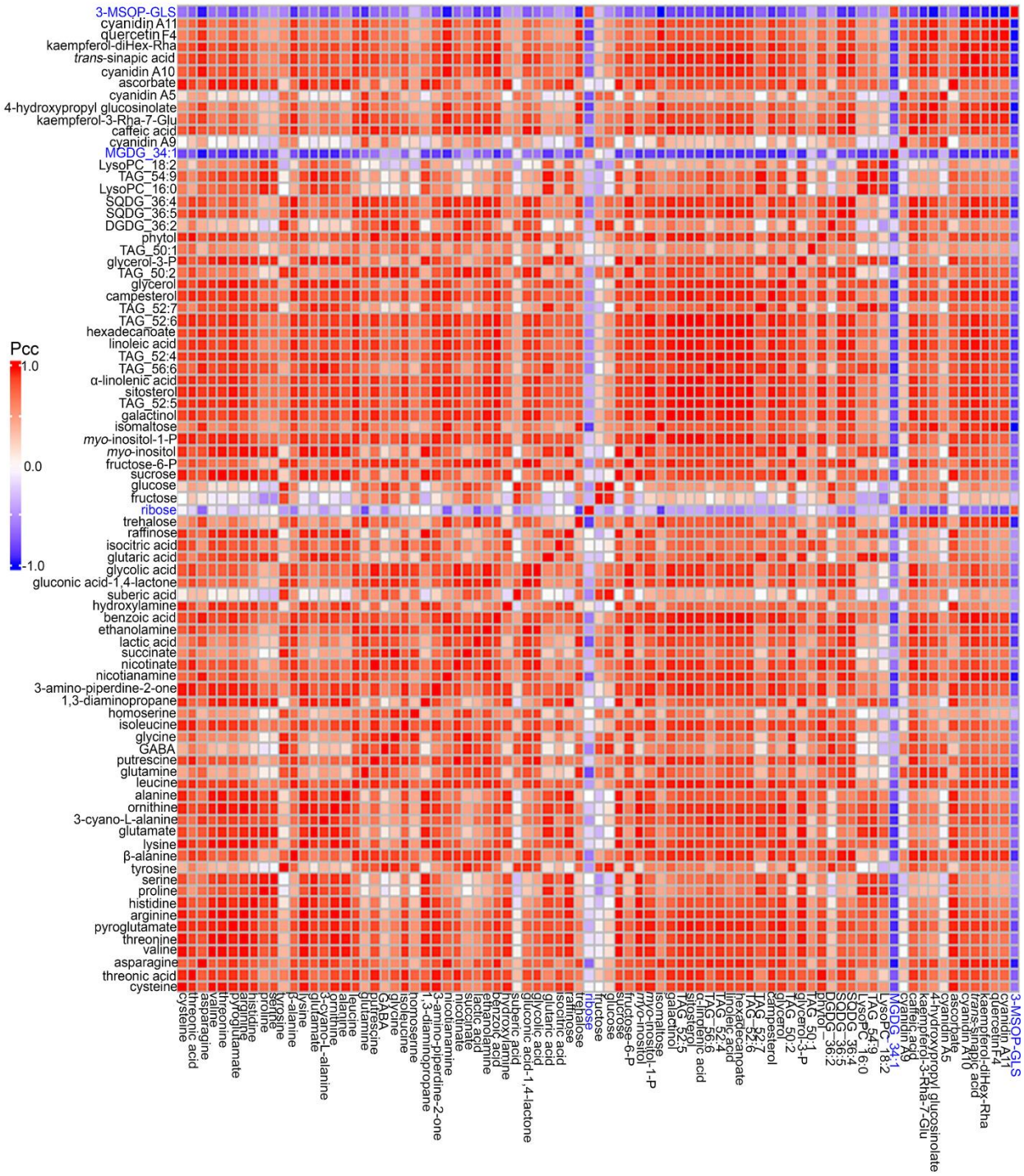

Fig. S3. Heatmap of 83 metabolites differentially produced in *ahp2,3,5* and *arr1,10,12* mutants, relative to wild-type plants (WT), grown under nonsaline ('*ahp2,3,5*-C/WT-C' and '*arr1,10,12*-C/WT-C') and saline ('*ahp2,3,5*-S/WT-S' and '*arr1,10,12*-S/WT-S' comparisons) conditions. Color scale indicates Pearson correlation coefficients (Pcc).

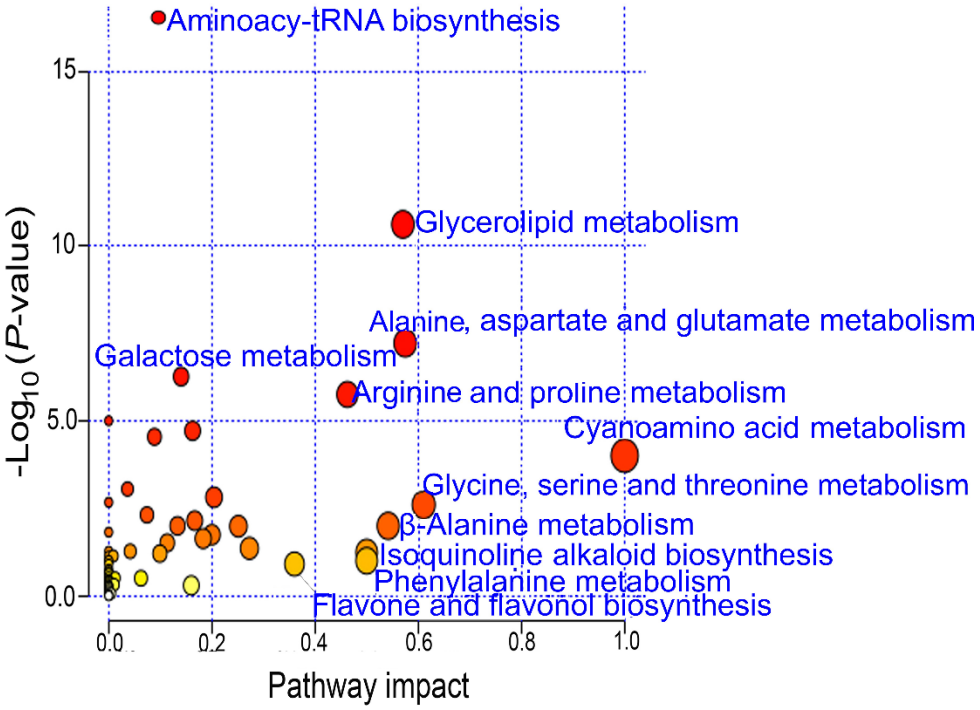

Fig. S4. Pathway enrichment analyses of 83 metabolites differentially produced in *ahp2,3,5* and *arr1,10,12* mutants, relative to wild-type (WT) plants, grown under nonsaline ('*ahp2,3,5*-C/WT-C' and '*arr1,10,12*-C/WT-C') and saline ('*ahp2,3,5*-S/WT-S' and '*arr1,10,12*-S/WT-S' comparisons) conditions. Red and yellow colors of the circles indicate high and low -$\log_{10}$ (*P*-values), respectively. The circle size indicates a high (larger circle) or low (smaller circle) pathway impact.

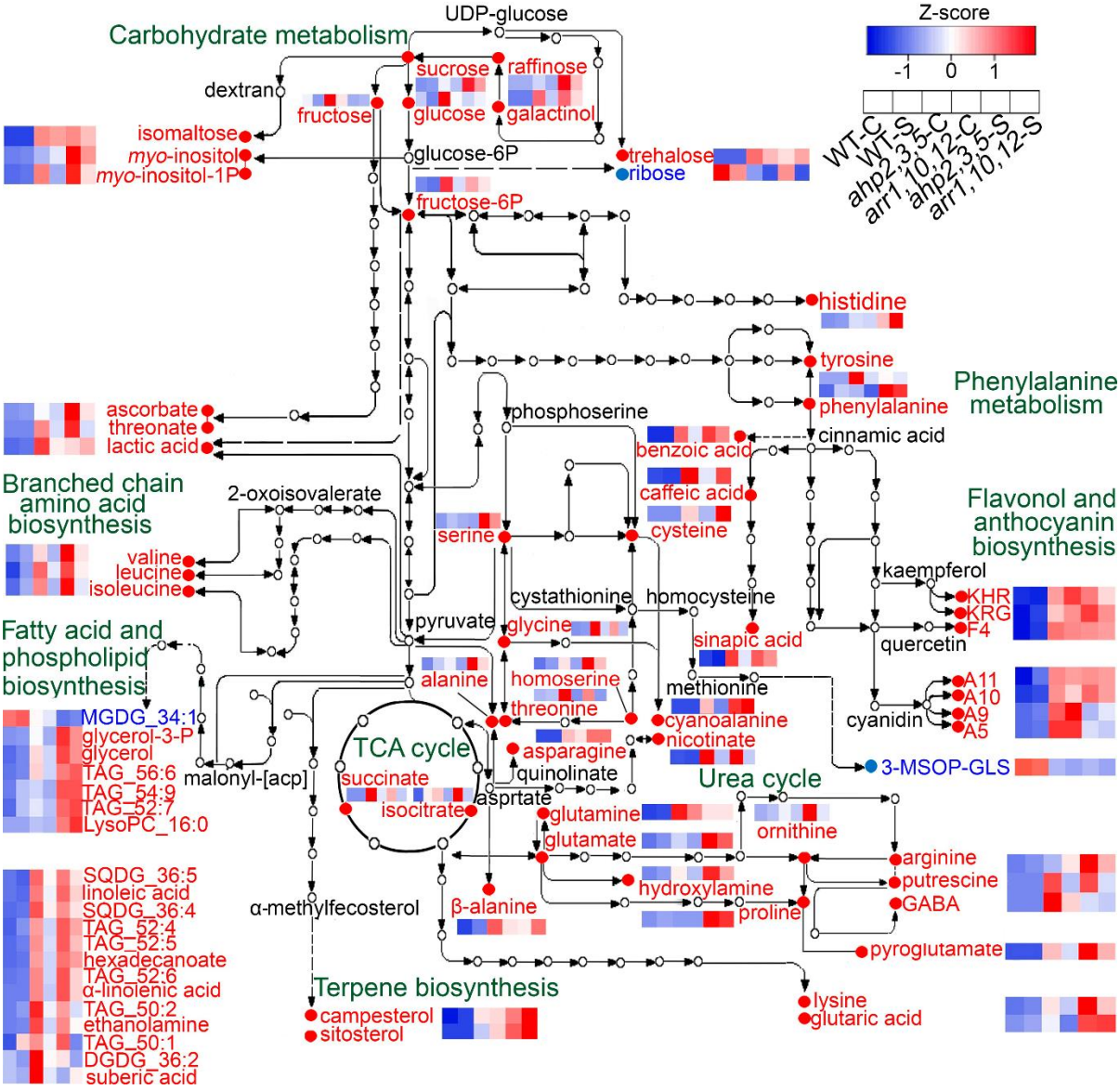

Fig. S5. Kyoto Encyclopedia of Genes and Genomes (KEGG) pathways associated with the 83 metabolites differently produced in *ahp2,3,5* and *arr1,10,12* mutants, relative to wild-type (WT) plants, grown under nonsaline ('*ahp2,3,5*-C/WT-C' and '*arr1,10,12*-C/WT-C') and saline ('*ahp2,3,5*-S/WT-S' and '*arr1,10,12*-S/WT-S' comparisons) conditions. The metabolite production levels in the heatmaps are a Z-score-normalized data matrix. KEGG IDs of the differentially produced metabolites were submitted to KEGG mapper to identify specific pathways. Red and blue colors indicate increased and decreased levels of metabolites, respectively, as indicated by the colored scales. γ-aminobutyric acid, GABA; cyanidin 3-*O*-[2-*O*-(β-D-xylopyranosyl)-6-*O*-(*E*-*p*-coumaroyl)-β-D-glucopyranoside]-5-*O*-[6-*O*-(malonyl)-β-D-glucopyranoside], A5; cyanidin 3-*O*-[2-*O*-(2-*O*-(*E*-sinapoyl)-β-D-xylopyranosyl)-6-*O*-(4-*O*-*E*-*p*-

coumaroyl)-β-D-glucopyranoside]-5-*O*-[6-*O*-(malonyl)-β-D-glucopyranoside], A9; cyanidin 3-*O*-[2-*O*-(2-*O*-(*E*-sinapoyl)-β-D-xylopyranosyl)-6-*O*-(4-*O*-(β-D-glucopyranosyl)-*E*-*p*-coumaroyl)-β-D-glucopyranoside]-5-*O*-[β-D-glucopyranoside], A10; cyanidin 3-*O*-[2-*O*-(2-*O*-(*E*-sinapoyl-β-D-xylopyranosyl)-6-*O*-(4-*O*-(β-D-glucopyranosyl)-(*E*-*p*-coumaroyl)-β-D-glucopyranoside)-5-*O*-[6-*O*-(malonyl)-β-D-glucopyranoside], A11; digalactosyldiacylglycerol, DGDG; kaempferol-diHex-Rha, KHR; kaempferol-3-Rha-7-Glu, KRG; lysophosphatidylcholine, LysoPC; monogalactosyldiacylglycerol, MGDG; quercetin-3-*O*-α-L-rhamnopyranosyl(1,2)-β-D-glucopyranoside-7-*O*-α-L-rhamnopyranoside, F4; rhamnoside, Rha; sulfoquinovosyl diacylglycerol, SQDG; triacylglycerol, TAG.

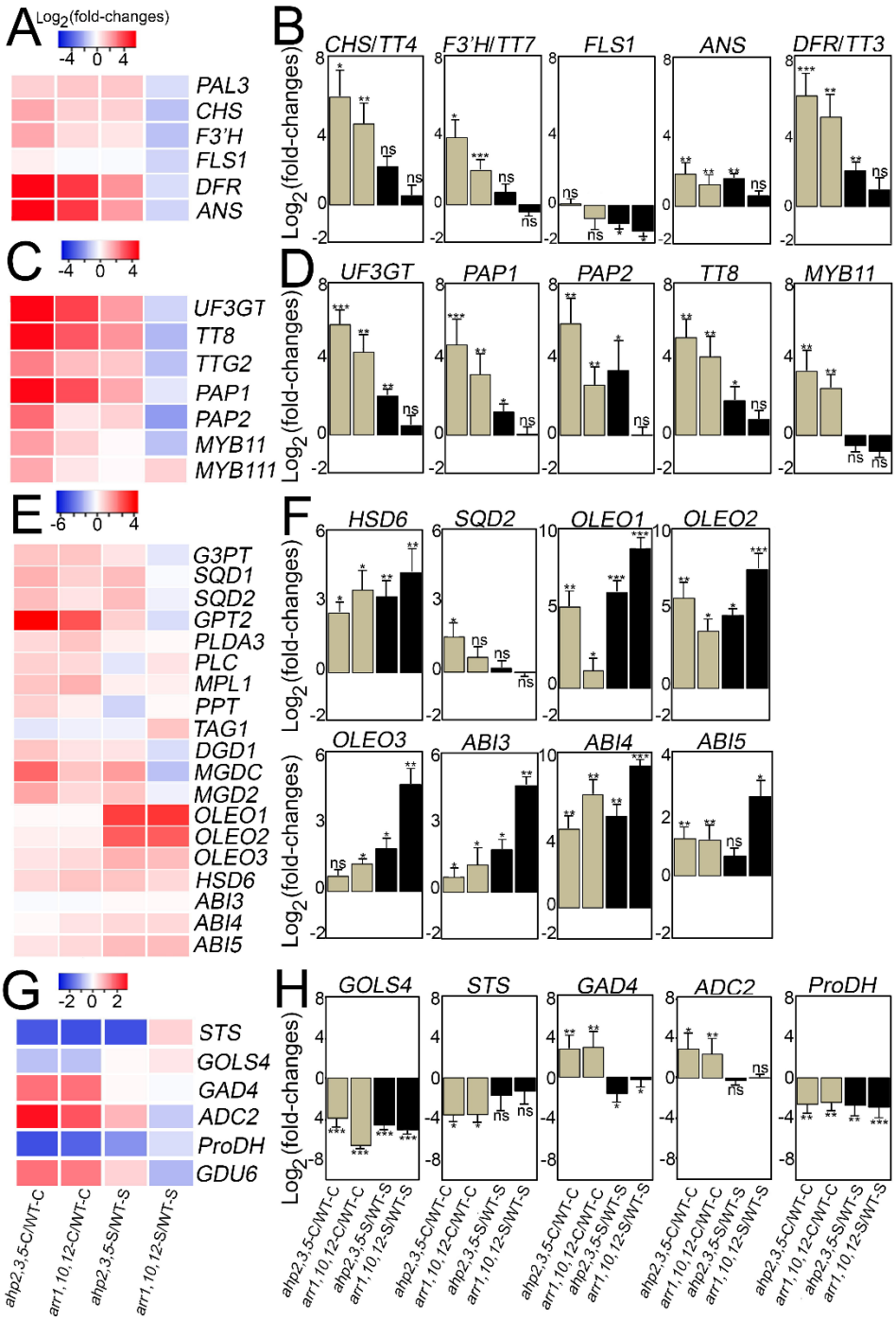

Fig. S6. Log_2 (fold-changes) in the expression of genes differentially expressed in *ahp2,3,5* and *arr1,10,12* mutants, relative to wild-type (WT) plants, grown under nonsaline ('*ahp2,3,5*-C/WT-C' and '*arr1,10,12*-C/WT-C') and saline ('*ahp2,3,5*-S/WT-S' and '*arr1,10,12*-S/WT-S' comparisons) conditions, as determined by transcriptome analysis (*A*, *C*, *E* and *G*) and reverse transcription-quantitative PCR (RT-qPCR) (*B*, *D*, *F* and *H*). Expression of flavonoid-related (*A-D*), lipid-related and sterol-related (*E-F*), and sugar-related and amino acid-related (*G-H*) genes

in the investigated comparisons. Data represents the means ± standard errors of three independent biological replicates (n = 3). Asterisks indicate significant fold-changes in each comparison according to a Student's t-test (*$P \leq 0.05$; **$P \leq 0.01$; ***$P \leq 0.001$). Non-significant, ns; *ABSCISIC ACID-INSENSETIVE*, *ABI*; *ARGININE DECARBOXYLASE 2*, *ADC2*; *CHALCONE SYNTHASE*/*TRANSPARENT TESTA 4*, *CHS*/*TT4*; *DIHYDROFLAVONOL 4-REDUCTASE*, *DFR*/*TT3*; *FLAVONOID 3'-MONOOXYGENASE*, *F3'H*; *FLAVONOL SYNTHASE*, *FLS*; *GALACTINOL SYNTHASE*, *GOLS4*; *GLUCOSE-6-PHOSPHATE/PHOSPHATE TRANSLOCATOR* 2, *GPT2*; *GLUTAMATE DECARBOXYLASE 4*, *GAD4*; *GLUTAMINE DUMPER 6*, *GUD6*; *GLYCEROL-3-PHOSPHATE TRANSPORTER/PERMERASE*, *G3PT*; *HYDROXYSTEROID DEHYDROGENASE 6*, *HSD6*; *LEUCOANTHOCYANIDIN DIOXYGENASE*/*ANTHOCYANIDIN SYNTHASE*, *LDOX*/*ANS*; *MYZUS PERSICAE-INDUCED LIPASE*, *MPL1*; *OLESINS*, *OLEO*; *PALMITOYL-PROTEIN THIOESTERASE*, *PPT*; *PHENYLALANINE AMMONIA LYASE3*, *PAL3*; *PHOSPHOLIPASE D ALPHA*, *PLDA*; *PHOSPHOLIPASE*/*CARBOXYLESTERASE*, *PLD*/*CXE*; *PRODUCTION OF ANTHOCYANIN PIGMENT 1*, *PAP1*/*MYB75*; *PAP2*/*MYB90*; *PROLINE DEHYDROGENASE*, *ProDH*; *STACHYOSE SYNTHASE*, *STS*; *UDP-SULFOQUINOVOSYL SYNTHASE*, *SQD*; *TRIACYLGLYCEROL BIOSYNTHESIS DEFECT 1*, *TAG1*; *TRANSPARENT TESTA 8*, *TT8*, *UDP-GLUCOSE:FLAVONOID 3-O-GLUCOSYLTRANSFERASE*, *UF3GT*.

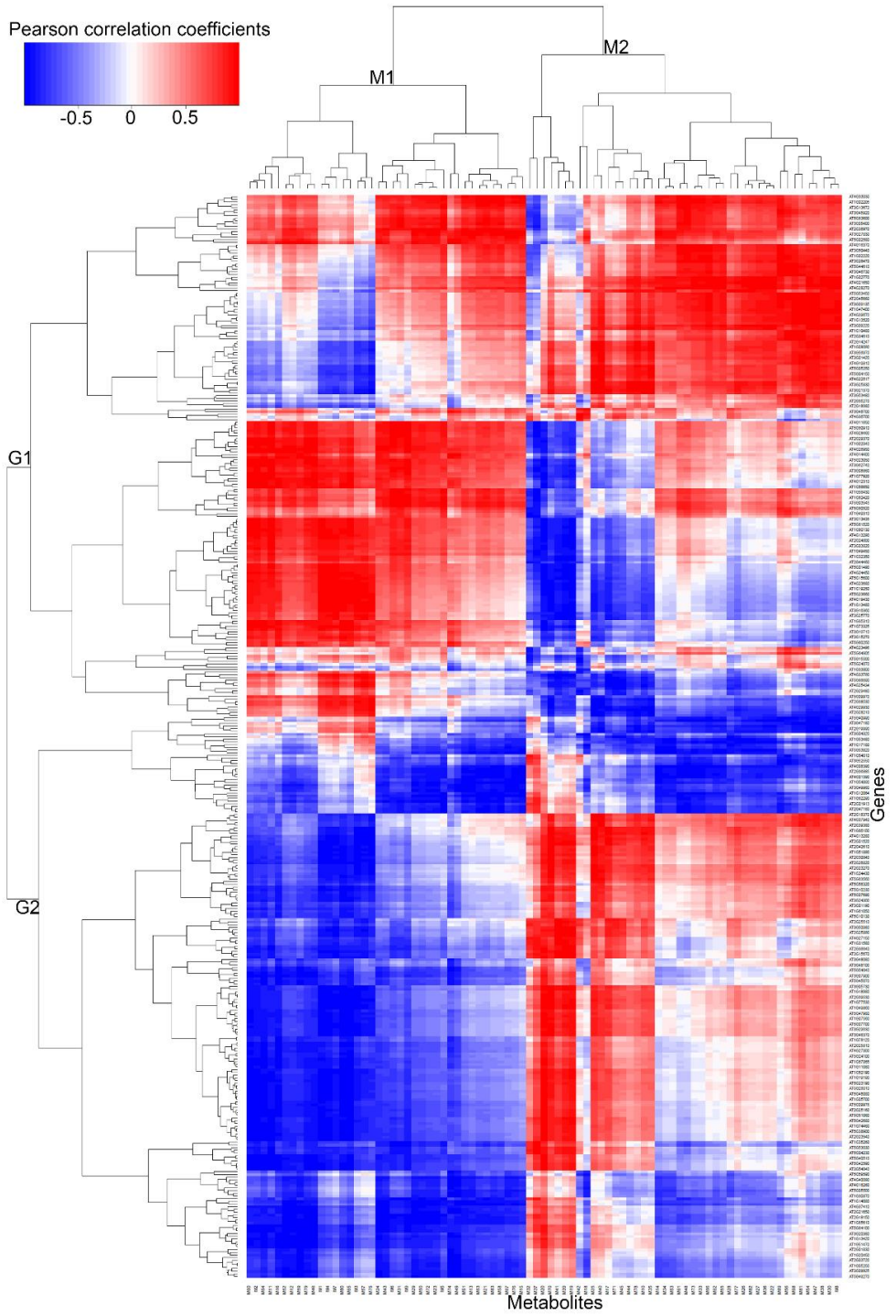

Fig. S7. 'Gene-metabolite' correlations of 403 overlapping differentially expressed genes and 83 overlapping differentially produced metabolites identified in *ahp2,3,5* and *arr1,10,12* mutants, relative to wild-type (WT) plants, grown under nonsaline ('*ahp2,3,5*-C/WT-C' and '*arr1,10,12*-C/WT-C') and saline ('*ahp2,3,5*-S/WT-S' and '*arr1,10,12*-S/WT-S' comparisons) conditions. Correlation analysis was estimated using the Pearson method, and the data (shown in **Dataset S10**) were used for heatmap clustering. Blue and red colors indicate negative and positive correlations, respectively.

Legends of Datasets

Dataset S1 (separate file). List of normalized primary and secondary metabolites successfully assigned, and their $\log_2$ (fold-changes) and false discovery rate (FDR) in *ahp2,3,5* and *arr1,10,12* mutants, relative to wild-type (WT) plants, grown under nonsaline ('*ahp2,3,5*-C/WT-C' and '*arr1,10,12*-C/WT-C') and saline ('*ahp2,3,5*-S/WT-S' and '*arr1,10,12*-S/WT-S') conditions, as well as for each genotype, under saline versus nonsaline conditions ('*ahp2,3,5*-S/*ahp2,3,5*-C', '*arr1,10,12*-S/*arr1,10,12*-C' and 'WT-S/WT-C' comparisons), as determined by gas chromatography time-of-flight mass spectrometry. Normalized data represent the means ± standard errors (SEs) of three biological replicates (n = 3).

Dataset S2 (separate file). List of normalized primary and secondary metabolites successfully assigned, and their $\log_2$ (fold-changes) and false discovery rate (FDR) in *ahp2,3,5* and *arr1,10,12* mutants, relative to wild-type (WT) plants, grown under nonsaline ('*ahp2,3,5*-C/WT-C' and '*arr1,10,12*-C/WT-C') and saline ('*ahp2,3,5*-S/WT-S' and '*arr1,10,12*-S/WT-S') conditions, as well as for each genotype, under saline versus nonsaline conditions ('*ahp2,3,5*-S/*ahp2,3,5*-C', '*arr1,10,12*-S/*arr1,10,12*-C' and 'WT-S/WT-C' comparisons), as determined by liquid chromatography quadruple time-of-flight mass spectrometry. Normalized data represent the means ± standard errors (SEs) of three biological replicates (n = 3).

Dataset S3 (separate file). List of normalized primary and secondary metabolites successfully assigned, and their $\log_2$ (fold-changes) and false discovery rate (FDR) in *ahp2,3,5* and *arr1,10,12* mutants, relative to wild-type (WT) plants, grown under nonsaline ('*ahp2,3,5*-C/WT-C' and '*arr1,10,12*-C/WT-C') and saline ('*ahp2,3,5*-S/WT-S' and '*arr1,10,12*-S/WT-S') conditions, as well as for each genotype, under saline versus nonsaline conditions ('*ahp2,3,5*-S/*ahp2,3,5*-C', '*arr1,10,12*-S/*arr1,10,12*-C' and 'WT-S/WT-C' comparisons), as determined by liquid chromatography quadruple time-of-flight mass spectrometry. Normalized data represent the means ± standard errors (SEs) of five biological replicates (n = 5).

Dataset S4 (separate file). Differentially produced metabolites [q-values ≤ 0.05; $\log_2$ (fold-changes) ≤ -1 and $\log_2$ (fold-changes) ≥ 1 for decreased and increased metabolites, respectively] in *ahp2,3,5* and *arr1,10,12* mutants, relative to wild-type (WT) plants, grown under nonsaline ('ahp2,3,5-C/WT-C' and '*arr1,10,12*-C/WT-C') and saline ('*ahp2,3,5*-S/WT-S' and '*arr1,10,12*-S/WT-S') conditions, as well as in each genotype under saline versus nonsaline conditions ('*ahp2,3,5*-S/*ahp2,3,5*-C' and '*arr1,10,12*-S/*arr1,10,12*-C' and 'WT-S/WT-C' comparisons). Red and blue colors indicate increased and decreased levels of metabolites, respectively, in different comparisons.

Dataset S5 (separate file). List of overlapping differentially produced metabolites [DPMs, q-values ≤ 0.05; $\log_2$ (fold-changes) ≤ -1 and $\log_2$ (fold-changes) ≥ 1 for decreased and increased metabolites, respectively] in different comparisons. (*A*) Overlapping DPMs in *ahp2,3,5* and *arr1,10,12* mutants, relative to wild-type (WT) plants, grown under nonsaline ('*ahp2,3,5*-C/WT-C' and '*arr1,10,12*-C/WT-C') and saline ('*ahp2,3,5*-S/WT-S' and '*arr1,10,12*-S/WT-S') conditions, as well as in each genotype under saline versus nonsaline conditions ('*ahp2,3,5*-S/*ahp2,3,5*-C', '*arr1,10,12*-S/*arr1,10,12*-C' and 'WT-S/WT-C' comparisons). (*B*) List of the 83 DMPs in the '*ahp2,3,5*-C/WT-C', '*arr1,10,12*-C/WT-C', '*ahp2,3,5*-S/WT-S' and/or '*arr1,10,12*-

S/WT-S' comparisons. Values represent metabolite $\log_2$ (fold-changes). Red and blue colors indicate overlapping increased and decreased levels of metabolites, respectively, in different comparisons.

Dataset S6 (separate file). 'Metabolite-metabolite' correlations of 83 metabolites differentially produced in the '*ahp2,3,5*-C/WT-C', '*arr1,10,12*-C/WT-C', '*ahp2,3,5*-S/WT-S' and/or '*arr1,10,12*-S/WT-S' comparisons. Correlation analysis was estimated using the Pearson method.

Dataset S7 (separate file). List of up-regulated [$\log_2$ (fold-changes) ≥ 1; *q*-values ≤ 0.05] and down-regulated [$\log_2$ (fold-changes) ≤ -1; *q*-values ≤ 0.05] genes in (*A*) the '*ahp2,3,5*-C/WT-C', (*B*) '*arr1,10,12*-C/WT-C', (*C*) '*ahp2,3,5*-S/WT-S', (*D*) '*arr1,10,12*-S/WT-S', (*E*) '*ahp2,3,5*-S/*ahp2,3,5*-C', (*F*) '*arr1,10,12*-S/*arr1,10,12*-C', and (*G*) 'WT-S/WT-C' comparisons. Red and blue colors indicate up-regulated and down-regulated genes, respectively.

Dataset S8 (separate file). Overlapping up-regulated [$\log_2$ (fold-changes) ≥ 1; *q*-values ≤ 0.05] and down-regulated [$\log_2$ (fold-changes) ≤ -1; *q*-values ≤ 0.05] genes in (*A*) the '*ahp2,3,5*-C/WT-C', '*arr1,10,12*-C/WT-C', '*ahp2,3,5*-S/WT-S' and '*arr1,10,12*-S/WT-S' comparisons, and (*B*) the 'WT-S/WT-C', '*ahp2,3,5*-S/*ahp2,3,5*-C' and '*arr1,10,12*-S/*arr1,10,12*-C' comparisons. Red and blue colors indicate overlapping up-regulated and down-regulated genes, respectively, in different comparisons.

Dataset S9 (separate file). (*A*) Overlapping up-regulated ($\log_2$ fold-changes ≥ 1; *q*-values ≤ 0.05) and down-regulated [$\log_2$ (fold-changes) ≤ -1; *q*-values ≤ 0.05] genes derived from *ahp2,3,5* and *arr1,10,12* mutants, relative to wild-type (WT) plants, grown under nonsaline and saline conditions. Red and blue colors indicate overlapping up-regulated and down-regulated genes, respectively. (*B*) 89 transcription factors potentially associated with salt tolerance of the mutant genotypes. (*C*) Eight transcription factor modules associated with the salt tolerance of the mutant genotypes.

Dataset S10 (separate file). 'Gene-metabolite' correlations of 403 overlapping differentially expressed genes and 83 overlapping differentially produced metabolites identified in *ahp2,3,5* and *arr1,10,12* mutants, relative to wild-type (WT) plants, grown under nonsaline ('*ahp2,3,5*-C/WT-C' and '*arr1,10,12*-C/WT-C') and saline ('*ahp2,3,5*-S/WT-S' and '*arr1,10,12*-S/WT-S' comparisons) conditions. Correlation analysis was estimated using the Pearson method.

Dataset S11 (separate file). List of the primers used in reverse transcription-quantitative PCR (RT-qPCR) analyses.